Evidence for Altered Spinal Canal Compliance and Cerebral Venous Drainage in Untreated Idiopathic Intracranial Hypertension

Noam Alperin, Byron L. Lam, Rong-Wen Tain, Sudarshan Ranganathan, Michael Letzing, Maria Bloom, Benny Alexander, Potyra R. Aroucha, and Evelyn Sklar

Abstract Idiopathic intracranial hypertension (IIH), or pseudotumor cerebri, is a debilitating neurological disorder characterized by elevated CSF pressure of unknown cause. IIH manifests as severe headaches, and visual impairments. Most typically, IIH prevails in overweight females of childbearing age and its incidence is rising in parallel with the obesity epidemic. The most accepted theory for the cause of IIH is reduced absorption of CSF due to elevated intracranial venous pressure. A comprehensive MRI study, which includes structural and physiological imaging, was applied to characterize morphological and physiological differences between a homogeneous cohort of female IIH patients and an age- and BMI-similar control group to further elucidate the underlying pathophysiology. A novel analysis of MRI measurements of blood and CSF flow to and from the cranial and spinal canal compartments employing lumped parameters modeling of the cranio-spinal biomechanics provided, for the first time, evidence for the involvement of the spinal canal compartment. The CSF space in the spinal canal is less confined by bony structures compared with the cranial CSF, thereby providing most of the craniospinal compliance. This study demonstrates that the contribution of spinal canal compliance in IIH is significantly reduced.

Keywords Intracranial hypertension • Underlying pathophysiology • Cranio-spinal biomechanical properties • Cerebral venous drainage • MRI CSF and blood flow studies

N. Alperin (✉), R.-W. Tain, S. Ranganathan, M. Letzing, M. Bloom, B. Alexander, and E. Sklar
Department of Radiology, Miller School of Medicine, University of Miami, 1150 N.W. 14th St., Suite 713, Miami, FL 33136, USA
e-mail: nalperin@med.miami.edu

B.L. Lam and P.R. Aroucha
Departments of Ophthalmology, Bascom Palmer Eye Institute, University of Miami, Miami, FL 33136, USA

Introduction

Idiopathic intracranial hypertension (IIH), or pseudotumor cerebri, is a debilitating neurological disorder characterized by elevated ICP of unknown cause. IIH manifests as severe headaches, and visual impairment due to increased pressure on the optic nerve. In addition to poor quality of life, IIH is associated with a considerable financial burden. Based on data from the IIH Registry, the total costs of IIH in 2007 in the US alone exceeded $444 million per year [8]. Most typically, IIH prevails in overweight females of childbearing age, with a high incidence of 22.5 new cases annually per 100,000, and is further rising in parallel with the obesity epidemic.

The origin and evolution of the disorder is not well understood, nor has evidence-based medicine identified an efficient and effective treatment path [7]. Often, individuals are diagnosed with IIH after all other possible identifiable causes have been exhausted. This occurs especially when prominent features such as papilledema and pulsatile tinnitus are not apparent [6], or if a marginally high opening pressure is obtained on lumbar puncture [4]. Currently, there is no established standard treatment for IIH. Treatment is primarily palliative, beginning with medical therapy and progressing to surgical therapy [3, 5]. Prescribed interventions include diet, diuretics, and carbonic anhydrase inhibitors, such as acetazolamide, repeated spinal taps, optic nerve sheath fenestration surgery, and CSF shunting procedures. The efficacy of each treatment varies among patients and the mechanism by which each treatment works is also not clear at present. Treatment often improves symptoms; however, 86% of patients suffer from some degree of permanent visual loss and 10% develop severe irreversible visual loss [15]. Better understanding of the pathophysiology is likely to improve this potentially devastating prognosis.

The most widely accepted theories on the causes of IIH are sinus venous focal narrowing and reduced absorption of CSF due to elevated intracranial venous pressure [10]. However, extra-cranial factors that may be contributing to the increased ICP in IIH and the adaptation of the cranio-spinal system have not been widely investigated.

M.U. Schuhmann and M. Czosnyka (eds.), *Intracranial Pressure and Brain Monitoring XIV*,
Acta Neurochirurgica Supplementum, Vol. 114, DOI: 10.1007/978-3-7091-0956-4_39, © Springer-Verlag/Wien 2012

The current study aims to investigate the potential involvement of extra-cranial venous drainage and the spinal canal compartment; the latter has not been previously considered as a contributor to the pathophysiology of IIH. As the spinal canal normally contributes to most of craniospinal compliance, it is likely that the elevated ICP is a manifestation of reduced compliance buffering in the spinal canal compartment.

Materials and Methods

Following approval by the Institutional Review Board and informed patient consent, 11 female patients (mean age, 29 ± 9 years; range, 17–44 years) with above-normal BMI (mean BMI, 35.4 ± 6.5 kg/m^2; range, 23.9–49.1) and 8 healthy women of comparable age (mean age, 32 ± 11; range, 22–50) and BMI (mean BMI, 37.1 ± 6; range, 30.9–48.5) were studied by MRI. The aim was to assess potential morphological and physiological differences between newly-diagnosed pretreated IIH patients and healthy subjects. Assessed parameters include gray matter, white matter, and ventricular volumes, total arterial inflow, venous outflow through primary (jugular veins) and secondary channels, estimated supratentorial CSF production rate, and spinal canal compliance contribution, all measured noninvasively by MRI.

Magnetic resonance imaging was obtained at 1.5 T (Siemens Healthcare). The MRI study included high-resolution 3D T1-weighted imaging for segmentation of the ventricular volumes and multiple velocities encoding phase contrast scans for imaging of the blood and CSF flows. High-velocity encoding of 70 cm/s was employed for imaging of blood flow dynamics to and from the cranial vault. Low velocity encoding of 12 and 7 cm/s was employed to image CSF flow through the aqueduct of Sylvius and between the cranium and the spinal canal respectively.

Imaging parameters for the T1-weighted structural brain scan included field of view (FOV) of 25.6 × 19.2 cm, acquisition matrix of 256 × 192, slice thickness of 1.0 mm, which provided 1-mm isotropic resolution. Imaging parameters for the phase contrast series used for imaging of the trans-cranial blood and CSF flows included FOV of 16 × 15.5 cm, acquisition matrix of 256 × 174 and slice thickness of 6 mm. A smaller FOV of 11 × 10 cm with slice thickness of 5.5 mm and acquisition matrix of 320 × 218 were used for imaging of the aqueductal flow. Minimum effective TR and TE (approximately 13–15 and 9 ms respectively) were always used for maximal temporal resolution.

Cerebral Venous Drainage

Venous drainage occurs through primary (e.g., internal jugular veins) and secondary (e.g., epidural, vertebral, deep cervical) venous channels. Mean volumetric flow rate in each internal jugular vein was calculated and added to obtain total venous drainage through the primary venous drainage channels. As total arterial inflow equals venous outflow, the relative cerebral venous drainage through the jugular veins was obtained by normalizing the total jugular flow with the total arterial inflow. Total arterial inflow, which is also the total cerebral blood flow (tCBF) is obtained by summation of mean volumetric flow rates through the two internal carotid and vertebral arteries. Volumetric flow rates were obtained by summation of the velocities within the blood vessel lumen area. Vessel lumen boundary was identified using the automated pulsatility-based segmentation method [1].

Morphological Assessment

The structural MR images of the brain were automatically segmented to extract the brain tissue for derivation of the intracranial volume using FSL software (Analysis Group, FMRIB, University of Oxford, Oxford, UK). The segmentation process uses a hidden Markov random field model based on image pixel intensity distribution [16]. Ventricular volumes were obtained by manual delineation of the ventricular boundaries by an experienced observer.

Cranio-Spinal Canal Compliance Distribution

A system analysis approach has been applied to estimate the cranio-spinal (CS) compliance distribution. A previously reported subject-specific lumped parameter model was employed to obtain the transfer function of the craniospinal system where the momentary difference between the arterial inflow and the venous outflow to and from the cranial vault is the input and the driving force for the cranio-spinal CSF pulsation, i.e., the output of the system [14]. A schematic representation of the compartmental model of the cranio-spinal system and an example of the MRI-derived waveform of blood and CSF flows demonstrating the input–output relationship between the blood and the CSF flow are shown in Fig. 1. The electrical circuit of the biomechanical analogous model includes the following lumped parameters: cranial and spinal compliance ($C1$ and $C2$ respectively), cranial and spinal CSF flow resistance ($R1$ and $R2$ respectively), and an

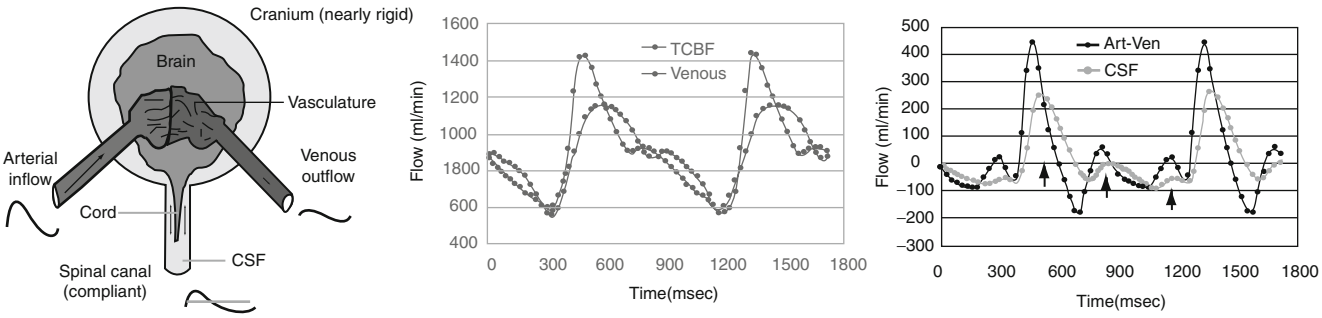

Fig. 1 The cranio-spinal system compartmental model employed to derive the cranio-spinal cerebrospinal fluid (CSF) compliance distribution. The arterial and venous volumetric flow rates are shown. The difference between these two waveforms (Art-Ven) is the driving force for the cranio-spinal CSF (*right*)

Table 1 Hemodynamic measures in idiopathic intracranial hemorrhage (IIH) and controls: mean and SD values of main hemodynamic parameters

	IIH ($n=11$)	Control ($n=8$)	p Value
Age (years)	28.6±8.9	31.8±9.9	0.49
BMI (kg/m^2)	34.2±5.1	36.4±5.8	0.38
Total cerebral blood flow (TCBF) (mL/min)	823±68	804±126	0.68
Total internal jugular flow (TIJF) (mL/min)	539±91[a]	634±84	0.03
Dominant IJF (mL/min)	385±111	430±104	0.39
Non-dominant IJF (mL/min)	148±68	209±78	0.08
TIJF/TCBF	0.65±0.08[a]	0.80±0.10	0.004

[a]Difference is statistically significant

inertia component ($I2$) to model the inertia-dominated CSF flow between the cranium and spinal canal [11]. The biomechanical characteristics of the CS system can be expressed by a transfer function, $H(s)$, shown in Eq. 1, which is the ratio of the Laplace transforms of the output (CSF flow waveform) to the input (arterial minus venous flow waveform).

$$H(s)=\frac{F_{csf}(s)}{F_{a-v}(s)}=\frac{\frac{R1}{I2}s+\frac{1}{I2\cdot C1}}{s^2+\frac{1}{I2}(R1+R2)s+\frac{1}{I2}\left(\frac{1}{C1}+\frac{1}{C2}\right)} \quad (1)$$

The ratio of the cranio and spinal canal compliance is then obtained by dividing the zero order coefficients in the numerator and denominator of the transfer function, as shown in Eq. 2.

$$\frac{C2}{C1+C2}=\frac{\frac{1}{I2\cdot C1}}{\frac{1}{I2}\left(\frac{1}{C1}+\frac{1}{C2}\right)} \quad (2)$$

Results

Mean and SD values of total cerebral blood flow (TCBF), total internal jugular flow (TIJF), flows through dominant internal jugular veins (DIJF), nondominant internal jugular veins (NIJF), and total internal jugular flow (TIJF) normalized to total cerebral blood flow are summarized in Table 1. Venous drainage through the primary venous channels is significantly reduced in IIH patient compared with healthy subjects. This difference is further enhanced after normalization with total cerebral blood flow as demonstrated by the smaller p value (p value <0.004). Example of a 3D MRV rendering of the extra-cranial venous vasculature from a control subject and from an IIH patient demonstrating the increased drainage through secondary channels in IIH is shown in Fig. 2. Means and SDs of morphological measures, CSF production rates and contribution to spinal canal compliance are summarized in Table 2. A trend toward slightly larger ventricular volumes in the IIH was observed. However, this trend was not statistically significant. No difference was found in CSF production rates between IIH and healthy. However, a larger but not significantly different variability in the CSF production was observed. In contrast to the morphological measures, spinal

Fig. 2 Example of Magnetic resonance venography of cervical venous drainage in a control subject (*left*) and an idiopathic intracranial hypertension (IIH) patient (*right*). In the healthy subjects, the venous drainage occurs mainly through the jugular veins (*arrows*) while in the IIH patients an increased drainage through the secondary venous channels (e.g., vertebral, deep cervical, epidural veins; *arrowheads*) is observed

Table 2 Intracranial morphology, CSF production rate, and compliance distribution in IIH and controls

	IIH ($n=11$)	Control ($n=8$)	p Value
Lateral ventricular volume (LVV) (cm^3)	16.5 ± 6.6	14.8 ± 5.5	0.57
Total ventricular volume (TVV) (cm^3)	18.5 ± 6.8	16.8 ± 5.7	0.56
Intracranial volume (ICV) (cm^3)	1374.2 ± 103.2	1335.6 ± 88.9	0.40
TVV/ICV (%)	1.34 ± 0.46	1.27 ± 0.47	0.74
Supratentorial CSF production rate (mL/min)	0.44 ± 0.28	0.44 ± 0.17[a]	0.99
Spinal canal compliance/total compliance	0.60 ± 0.12[b]	0.75 ± 0.09	0.026

[a]SD of CSF production is not significantly different, $p=0.13$
[b]Difference is statistically significant

canal compliance contribution is significantly different in IIH and controls. A significantly smaller contribution to spinal canal compliance (0.6 vs. 0.75) was found in IIH ($p=0.026$).

Discussion

An MRI-based comprehensive characterization of the cerebral hemodynamics, venous drainage, cerebral ventricular morphology, and cranio-spinal compliance distribution was applied to homogeneous cohorts of pretreated female IIH subjects and an age- and BMI-similar group of healthy women. Several significant differences that further elucidate the pathophysiology of IIH have been identified. The most significant finding of this study is a contribution to lower spinal canal compliance in IIH. Mechanical compliance represents the ability of a compartment to accommodate an increase in volume without a large increase in pressure. A subject-specific assessment of the relative contribution of the spinal canal to the overall cranio-spinal compliance based on the relationship of the blood flow and cranio-spinal CSF flow reveals that spinal canal compliance buffering is significantly reduced in IIH.

Conclusion

This finding suggests, for the first time, that the spinal canal plays an important role in the pathophysiology of IIH. It has been documented that ICP fluctuates considerably over a short period of time in IIH. As the spinal canal provides most

of the buffering for increased CSF volume, reduced spinal canal compliance buffering provides a good explanation of the impaired regulation of CSF pressure in IIH. This finding further explains why obesity carries an increased risk of IIH. Hogan et al. reported significantly smaller CSF space cross-sectional areas in obese compared with slim subjects. They attributed the smaller CSF area to inward displacement of the neural foraminal contents caused by high abdominal pressure [9]. Therefore, the already compressed spinal canal CSF space in obese subjects is very likely increasing resistance for expansion, thereby reducing the spinal canal compliance buffering. The second important observation of reduced cerebral venous drainage through the primary venous channels is in agreement with an earlier report of increased drainage through secondary venous channels in IIH [2]. As previously suggested, this may reflect increased resistance to venous drainage in IIH.

Conflict of interest statement We declare that we have no conflict of interest.

References

1. Alperin N, Lee SH (2003) PUBS: pulsatility-based segmentation of lumens conducting non-steady flow. Magn Reson Med 49:934–944
2. Alperin N, Lee SH, Mazda M, Hushek SG, Roitberg B, Goodwin J (2005) Evidence of the importance of extracranial venous flow in patients with Idiopathic Intracranial Hypertension (IIH). Acta Neurochir Suppl 95:129–132
3. Ball AK, Clark CE (2006) Idiopathic intracranial hypertension. Lancet Neurol 5:433–442
4. Bono F, Cristiano D, Mastrandrea C, Latorre V, D'Asero S, Salvino D, Fera F, Lavano A, Quattrone A (2010) The upper limit of normal CSF opening pressure is related to bilateral transverse sinus stenosis in headache sufferers. Cephalalgia 30:145–151
5. Digre KB (1999) Idiopathic intracranial hypertension. Curr Treat Options Neurol 1:74–81
6. Digre KB, Nakamoto BK, Warner JEA, Langeberg J, Baggaley SK, Katz BJ (2009) A comparison of idiopathic intracranial hypertension with and without papilledema. Headache 49:185–193
7. Friedman DI (2007) Idiopathic intracranial hypertension. Curr Pain Headache Rep 11:62–68
8. Friesner D, Rosenman R, Lobb BM, Tanne E (2010) Idiopathic intracranial hypertension in the USA: the role of obesity in establishing prevalence and healthcare costs. Obes Rev 12(5):1–8
9. Hogan QH, Prost R, Kulier A, Taylor ML, Liu S, Leighton M (1996) Magnetic resonance imaging of the cerebrospinal fluid volume and the influence of body habitus and abdominal pressure. Anesthesiology 84:1341–1349
10. Karahalios DG, Rekate HL, Khayata MH, Apostolides PJ (1996) Elevated intracranial venous pressure as a universal mechanism in pseudotumor cerebri of varying etiologies. Neurology 46:198–202
11. Loth F, Yardimci M, Alperin N (2001) Hydrodynamic modeling of cerebrospinal fluid motion within the spinal cavity. J Biomech Eng 123:71–79
12. Reid AC, Matheson MS, Teasdale G (1980) Volume of the ventricles in benign intracranial hypertension. Lancet 316:7–8
13. Reid AC, Teasdale GM, Matheson MS, Teasdale EM (1981) Serial ventricular volume measurements: further insights into the aetiology and pathogenesis of benign intracranial hypertension. J Neurol Neurosurg Psychiatry 44:636–640
14. Tain R, Alperin N (2009) Noninvasive intracranial compliance from MRI-based measurements of transcranial blood and CSF flows: indirect versus direct approach. IEEE Trans Biomed Eng 56:544–551
15. Wall M, George D (1991) Idiopathic intracranial hypertension: a prospective study of 50 patients. Brain 114:155–180
16. Zhang Y, Brady M, Smith S (2001) Segmentation of brain MR images through a hidden Markov random field model and the expectation maximization algorithm. IEEE Trans Med Imaging 20:45–57